



Capture of Lead Ions from Aqueous Solution by Mg/Fe-LDH Alginate Beads Prepared from *Schanginia aegyptiaca* and Scrap Iron

Zainab Y. Al-Rubaie*^{ID}, Ayad A.H. Faisal^{ID}

Department of Environmental Engineering, College of Engineering, University of Baghdad, Baghdad 10011, Iraq

Corresponding Author Email: zainab.yahia2111p@coeng.uobaghdad.edu.iq

Copyright: ©2025 The authors. This article is published by IETA and is licensed under the CC BY 4.0 license (<http://creativecommons.org/licenses/by/4.0/>).

<https://doi.org/10.18280/ijdne.200315>

ABSTRACT

Received: 1 January 2025

Revised: 1 March 2025

Accepted: 10 March 2025

Available online: 31 March 2025

Keywords:

lead, Schanginia aegyptiaca, sorption, scrap iron, nanocomposites

This study aims to develop a novel sorbent using solid waste from scrap iron and *Schanginia aegyptiaca*. Magnesium and iron ions can be efficiently extracted from solutions derived from *Salsola aegyptiaca* and scrap iron, respectively. Sodium alginate beads are used to immobilize magnesium-iron nanoparticles. Using batch adsorption experiments, the prepared sorbent, termed magnesium/iron-layered double hydroxide-sodium alginate beads (Mg/Fe-LDH-Na alginate beads), was tested for its ability to remove lead (Pb) ions from simulated wastewater. The optimal conditions for synthesizing the Mg/Fe-LDH beads were determined to be 3, 10, and 5 g, corresponding to the molar ratio, pH, and dosage, respectively. The best operating parameters were 120 minutes, initial pH 6, 0.5 grams of beads per 100 mL, and 250 rpm for an initial concentration (C_0) of 10 mg/L to remove more than 90% of Pb^{2+} ions. The reuse performance of the sorbent was evaluated under the same batch test conditions and Pb removal efficiency was 95.9% in the first cycle, decreasing to approximately 84.7% by the sixth cycle, indicating a decline in removal efficiency with repeated use. The sorption process is well described by the Langmuir model, which suggests a maximum adsorption capacity of 2.312 mg/g. The results indicate that the produced beads are highly reusable and reliable, making them useful for removing lead ions from water, particularly in practical applications.

1. INTRODUCTION

Heavy metals are metallic elements characterized by high density and toxicity. Their presence poses significant environmental risks. These metals are primarily introduced into water sources through industrial activities, urbanization, and natural processes. Metals typically detected in water include lead, mercury, cadmium, arsenic, nickel, chromium, and zinc [1-3]. Furthermore, understanding the sources of lead exposure and the signs of lead poisoning is important for prevention and early intervention. If lead exposure is suspected, clinical evaluation and blood testing are essential for proper diagnosis and management [4-8]. Lead removal from water can be achieved using various techniques, including chemical precipitation, electrochemical methods, sorption, and membrane separation. Sorption is essential for treating lead-containing solutions due to its simplicity, efficiency, and low cost [9-11].

The choice of sorbents is crucial, as these materials should be cost-effective, durable, efficient, and environmentally friendly [12, 13]. Various sorbents have been utilized in previous studies to remove lead from solutions, such as activated carbon [14], clay [15, 16], and montmorillonite [17]. Therefore, developing innovative sorbents that satisfy the aforementioned criteria is essential. Nanoparticles are highly effective for removing lead ions due to their tunable surfaces,

abundant binding sites, and rapid adsorption kinetics [18, 19]. Notably, those derived from solid wastes serve as environmentally friendly sorbents [20, 21]. Magnetic chitosan [22-24] are examples of nanoparticle materials.

LDHs are ionic lamellar compounds characterized by positively charged layers, similar to brucite, which can be separated by interlayer molecules. Cations are situated at the centers of side-sharing octahedra, which are surrounded by hydroxide ions that connect to create continuous two-dimensional sheets. However, the structure of LDHs can restrict their sorption capacity due to the dense stacking of these multi-layered sheets [25]. LDHs have been synthesized and applied as sorbents for the removal of various heavy metals. For instance, co-precipitation was employed to create core-shell Fe_3O_4 -LDHs, which was analyzed for its sorption capabilities [26]. The Fe/Mg/Ni-LDH, a highly selective and sensitive nanomaterial, was investigated for detecting lead ions electrochemically using rectangular wave anodic stripping voltammetry [27]. The magnetic alginate microspheres containing Fe_3O_4 /MgAl-LDH were developed and immobilized within calcium alginate to effectively remove cadmium, lead, and copper [28]. Innovations in this field include the development of new LDH adsorbents, such as MgCuCaAl-LDH, which have been investigated for their thermodynamic properties in Pb^{2+} removal [29]. Additionally, composites like MIL-101(Fe)@MgFe-LDH have been

designed for the simultaneous mineralization of multiple heavy metals, including Pb^{2+} , Cd^{2+} , and Cu^{2+} [30]. Green techniques for synthesizing LDHs play an important role in minimizing environmental impact while enhancing their functionality and applicability. These techniques consist of the use of agents [31], hydrothermal synthesis [32], eco-friendly co-precipitation [33], and extracting metals from waste materials [31, 33].

Schanganina (SC) is a common plant in Iraq and other arid regions, recognized for its high magnesium content and the presence of various bioactive compounds, including flavonoids, alkaloids, saponins, tannins, and glycosides [34]. Additionally, iron scrap (IS) is generated daily in various industrial workshops across Iraq, with each workshop discharging an average of approximately 1.2 tons of scrap iron per day [35]. This study investigates the preparation of Mg/Fe-LDH alginate beads using SC and IS. The efficiency of the synthesized beads will be evaluated for lead removal from aqueous solutions [36].

2. SORPTION DATA MODELING

2.1 Sorption isotherms

Sorption is the relation between the contaminant molecules retained by the sorbent (q_e , mg/g) and the molecules' remaining concentration at equilibrium (C_e , mg/L), and "sorption isotherm" can represent such a relationship at a constant temperature. To evaluate the reactive material, the constant of "sorption isotherm" must be calculated, especially the "maximum adsorption capacity, q_m " which reflects the milligrams number of contaminants retained per one gram of solid material (Weber and Morris, 1962). An advantageous isotherm is convex upward, permitting relatively high sorption at low contaminant concentration. A summary of the sorption isotherm models employed to formulate the sorption data of this research is listed as follows:

a. Freundlich model: Freundlich and Kuster in 1894 published the first nonlinear form of an isotherm which could be expressed in the following form [37]:

$$q_e = K_f C_e^{1/n} \quad (1)$$

The Freundlich constants, K_f (mg/g)(L/mg)^(1/n) and n , are associated with the sorption capacity and sorption intensity, respectively.

b. Langmuir model: One of the isotherm relationships published by Irving Langmuir in 1916 as a new nonlinear model for redistribution of chemicals between solid-liquid phases, and it bears his name. The monolayer of contaminant molecules is accumulated on the sorbent surface. Maximum sorption, constant sorption energy, and no solute transmigration in the surface plane are popular assumptions applied to derive this isotherm. Langmuir isotherm is written as below [37]:

$$q_e = \frac{q_m b C_e}{1 + b C_e} \quad (2)$$

where, b represents the contaminant affinity towards the sorbent (L/mg).

2.2 Kinetics models

Kinetics refers to the rate of contaminant uptake, which

influences the sorbate residence time at the solid-solution interface. Understanding this rate is essential for elucidating the mechanisms of the sorption process. Therefore, predicting how quickly solutes are removed from water is crucial for designing an effective sorption treatment system [38]. To clarify the sorption mechanism and identify the potentially dominant stages, the following two kinetic models should be applied:

a) "Pseudo-first order kinetic model": Lagergren (1989) formulated the rate equation for the sorption process. This model takes the following form:

$$q_t = q_e(1 - e^{-k_1 t}) \quad (3)$$

where, q_e is the sorption capacity at equilibrium (mg/g), k_1 is the rate constant (min^{-1}), and q_t is the sorption capacity at time t (mg/g).

b) "Pseudo-second order kinetic model" is described based on certain assumptions [39]; a) Formation of a single layer of solute on the sorbent surface, b) All sorbent particles have the same sorption energy regardless of the extent of surface coverage, and c) Sorption occurs at specific sites where no interaction takes place between the adsorbed solute molecules, and the sorption rate is negligible compared to the initial rate. The following equation defines this model:

$$q_t = \frac{t}{\left(\frac{1}{k_2 q_e^2} + \frac{t}{q_e}\right)} \quad (4)$$

3. EXPERIMENTAL WORK

3.1 Materials and Methods

Chemicals with high purity were utilized, including hydrochloric acid (HCl), sodium hydroxide (NaOH) pellets, calcium chloride ($CaCl_2$), and sodium alginate ($NaC_6H_7O_6$, molecular weight 2.5×10^5 g/mol) supplied by Sigma Aldrich, USA. Lead was selected to simulate contamination in water. The contaminated water was prepared by dissolving $PbCl_2$ (from Thomas Baker) in distilled water (DW) to obtain 1000 mg Pb in one liter of aqueous solution, which is considered a "stock solution" for achieving the required concentration. The pH adjustments (SD300pH, Lovi bond, Germany) were conducted by the addition of 0.1 M sodium hydroxide (NaOH) or hydrochloric acid (HCl) as needed. The concentration of lead is measured by "Atomic Absorption Spectroscopy (AA-7000, Shimadzu, Japan)".

3.2 Manufacturing of beads

The initial step in synthesizing adsorbent involves magnesium extraction from Schanganina (SC) and iron from scrap iron (IS). The extracted metal ions were immobilized with sodium alginate as the following:

1. The wastes of SC were collected from the rural areas of Madhatiya city in Babylon Governorate-Iraq. Stem, leaves, and fruits were dried for a certain period under the sun. Because the plant contains a high-water content, it was also dried in the oven at 85 degrees Celsius. It was ground in a mechanical mill and sieved. The SC was immersed in hot water and washed with distilled water (DW) to detach residual fat and impurities, dried at 105°C (Herathern OGS60, Thermo Scientific, Germany), and then, the SC must be grounded to be

a powder. To extract the highest concentration of Mg ions from the SC plant, various dosages of SC (3-20 g) and various HCl concentrations (2-14%) were tested under the agitation of 250 rpm (HY-4, Triup International Corp, Italy) for 3 hours at 20°C. The 20 grams of SC per 300 mL of aqueous solution contained 4% hydrochloric acid optimized to be the best value to extract 7440 mg/L highest concentration of Mg ions.

2. SI was obtained from workshops in Hillah, Iraq. Preliminary tests demonstrated that adding 5 g of IS to 300 mL of an aqueous solution containing 4% HCl, under agitation at 250 rpm for 3 hours, was sufficient to extract an iron concentration of 410451 mg/Filter papers have been used to separate the particles from the solution.

3. To determine the pH (7-12), the magnesium and iron solutions were mixed with different molar ratios (Mg/Fe) with a range (0.5- 5) and precipitated by changing the pH with 1 M sodium hydroxide and under conditions stirring speed= 250 rpm, stirring duration= 3 hours, and temperature at room temperature (25 ± 5°C). Following agitation, precipitates were generated, separated, dried at 85°C, washed with DW, dried for 8 hours at 200°C, and then crushed into a powder.

4. A sodium alginate solution was prepared by dissolving 2 g of Na-alginate in 100 mL of distilled water and stirring continuously for 24 hours. The generated solution has been supplemented with various amounts of nanoparticles, and to create beads, the slurry needs to be added to 0.1 M CaCl₂.

At 105°C, the beads were dry. Figure 1 shows the steps involved in the preparation, and the best conditions for synthesis were identified based on how well the produced beads removed Pb ions.

3.3 Batch adsorption experiments

The adsorption equilibrium and kinetics of Pb ions onto the adsorbent were tested in batch adsorption experiments. The tests aim to determine the optimal time, agitation speed, pH, and dosage of adsorbent at a given C₀. A specific volume of aqueous solution (V=100 mL) is added to flasks that have been prepared. A specific mass of the prepared beads (m) is mixed with the contaminated water in the flasks, which are then shaken for three hours at 250 rpm. After agitation, the beads need to be separated using filter paper, and "Atomic Absorption Spectroscopy (AA-7000, Shimadzu, Japan)" is utilized to measure the equilibrium Pb concentration (C_e). Eq. (5) can be used to determine the concentration of Pb adsorbed at equilibrium (q_e). C₀ (5–200 mg/L), pH (3–10), duration (0–240 min), agitation speed (50–300 rpm), and sorbent mass (0.1–1) g/100 mL were all used in the tests [40].

$$q_e = (C_o - C_e) \frac{V}{m} \quad (5)$$

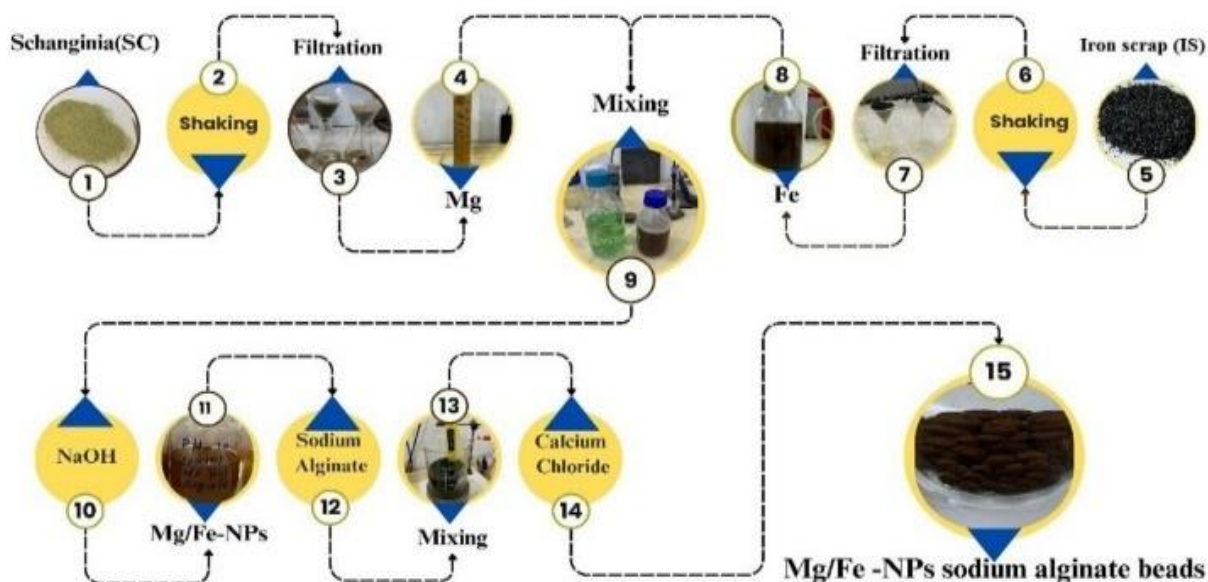


Figure 1. Schematic representation of the synthesis adsorbent (Mg/Fe-LDH-sodium alginate)

4. RESULTS AND DISCUSSION

4.1 Synthesis of beads

At pH 7–12, with an LDH nanoparticle mass of 5 grams per 100 milliliters and an Mg: Fe molar ratio of 1:1, the effect of initial pH on adsorbent production was investigated. A 50 mL with 10 mg/L of C₀ for Pb ions at initial pH 7, 250 rpm agitation, and a 3-hour contact duration was combined with 0.5 grams of beads for the sorption tests. Figure 2(a) clearly shows that varying pH (7-12) caused the adsorption capacity of adsorbent for Pb ions to fluctuate between 0.84 and 1.46 mg/g, and the maximum value (1.6 mg/g) was achieved at

pH=10. The impact of different molar ratios (Mg/Fe) on the adsorption capacity of adsorbent was investigated. The adsorption tests were conducted under identical conditions as described, with a pH of 10 and a nanoparticle dosage of 5 g/100 mL for synthesis. The variation in Mg/Fe from 0.5 to 5 caused the Pb adsorption capabilities to vary from 1.38 to 1.42 mg/g, as shown in Figure 2(b). The results demonstrate that the highest Pb adsorption capacity (1.838 mg/g) is attained at an Mg/Fe molar ratio of 3. The dosage of nanoparticles was varied (0.5- 5 g/100 mL) at 10 and 3 for pH and molar ratio, respectively (Figure 2(c)). The findings show that increasing the nanoparticle mass from 0.5 to 5 g/100 mL results in an increase in Pb adsorption capacity from 1.38 to 1.85 mg/g.

4.2 Batch adsorption experiments

One important step in finding the Pb ions distribution between the beads and aqueous solution in batch adsorption experiments is the contact time needed to reach the equilibrium condition. Figure 3(a) illustrates the Pb ion adsorption efficiency over 240 min at pH 5, speed = 250 rpm, an adsorbent mass = 0.5 g/100 mL, and $C_o = 10$ mg/L. The metal is rapidly removed for up to 120 minutes, after which it is significantly diminished since fewer binding sites are present. The Pb ions sorption efficiency is 88%, and it essentially stabilizes until 240 minutes. The dependence of Pb's capture efficiency on C_o is demonstrated in Figure 3(b). Due to the change in C_o (5 - 200 mg/L) with pH 5, a dose of 0.5 g/100 mL, and 250 rpm, the adsorption efficiency significantly decreased from 89.8% to 33%. It is anticipated that at lower contaminant concentrations, all of Pb will interact with the accessible sites, resulting in a marked improvement in sorption efficiency. However, increased Pb brought on by an increase in metal concentration for a certain gram of beads could cause this efficiency to decrease [41].

One important factor in improving Pb ion removal is the rate of agitation. Figure 3(c) illustrates how agitation speed affects

the effectiveness of metal elimination. It has been observed that as speed increases, removal efficiency can increase dramatically. The Pb and the available sites can form a suitable relationship since the increased agitation speed facilitates the metal's diffusion through the adsorbent. The observed data indicate that an agitation speed of 250 rpm is sufficient to achieve maximum lead ion removal (91.4%), with no significant variation in removal efficiency beyond this speed [42].

Another crucial factor to take into account is the aqueous solution's pH, which has a significant impact on the removed Pb. This necessitates conducting experiments using predetermined initial pH ranges, namely 3 to 6, and stabilizing other operational parameters, as illustrated in Figure 3(d). The Pb removal percentage improved significantly with increasing pH up to a pH of 6; beyond this, experiments were not conducted to avoid precipitation. The following is the cause of this behavior: Due to competition between the metal ions and H^+ for the sorption sites on the bead surface, the lead removal percentage was low at pH 3 (=32%). The percentage of elimination increased with higher pH, peaking at 91.9% for pH 6 due to the decrease in the hydrogen ions [43, 44].

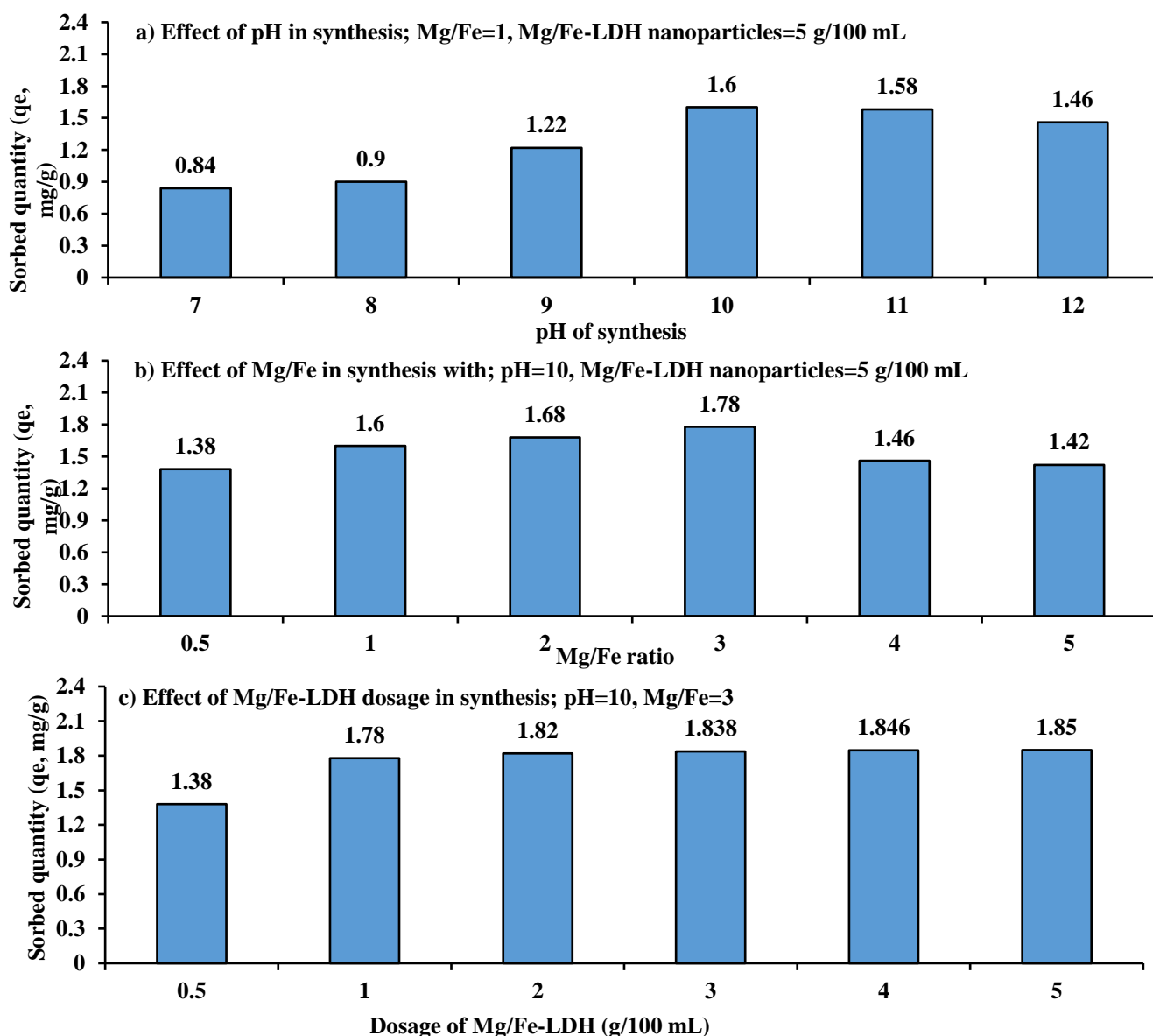
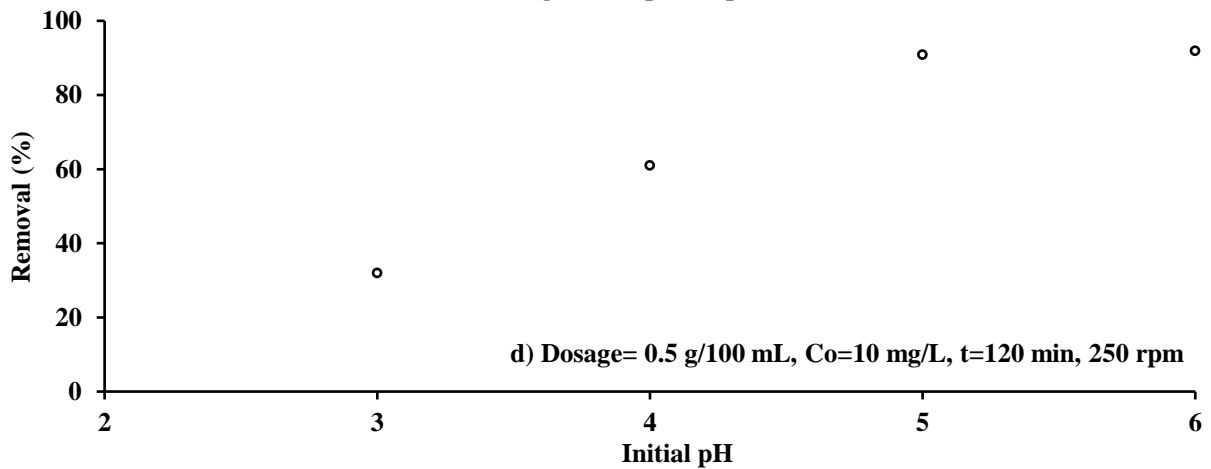
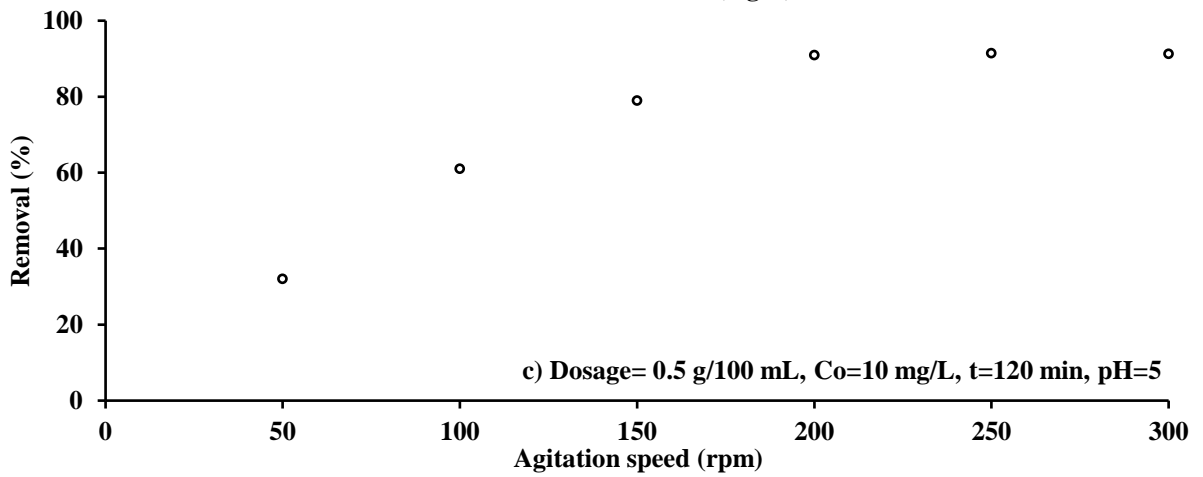
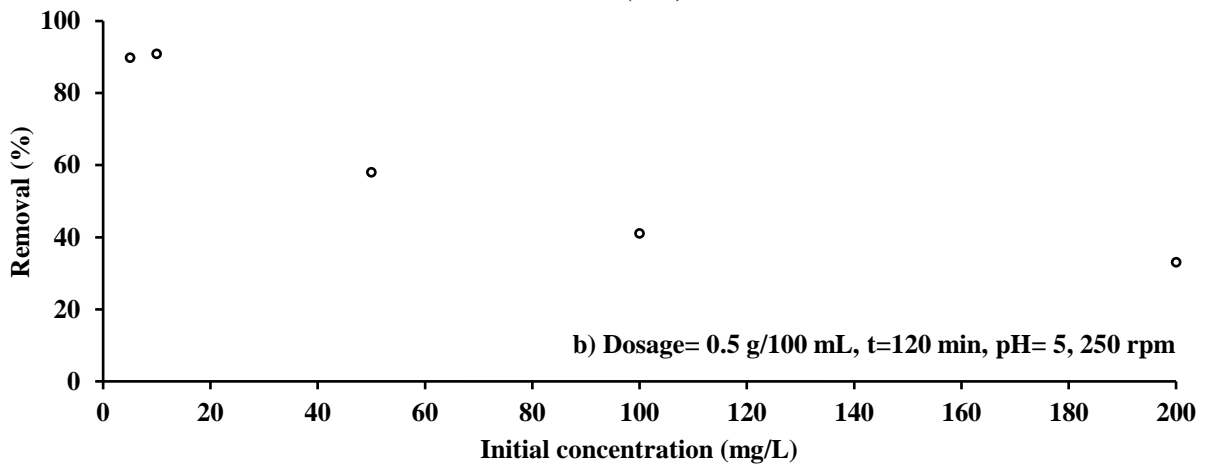
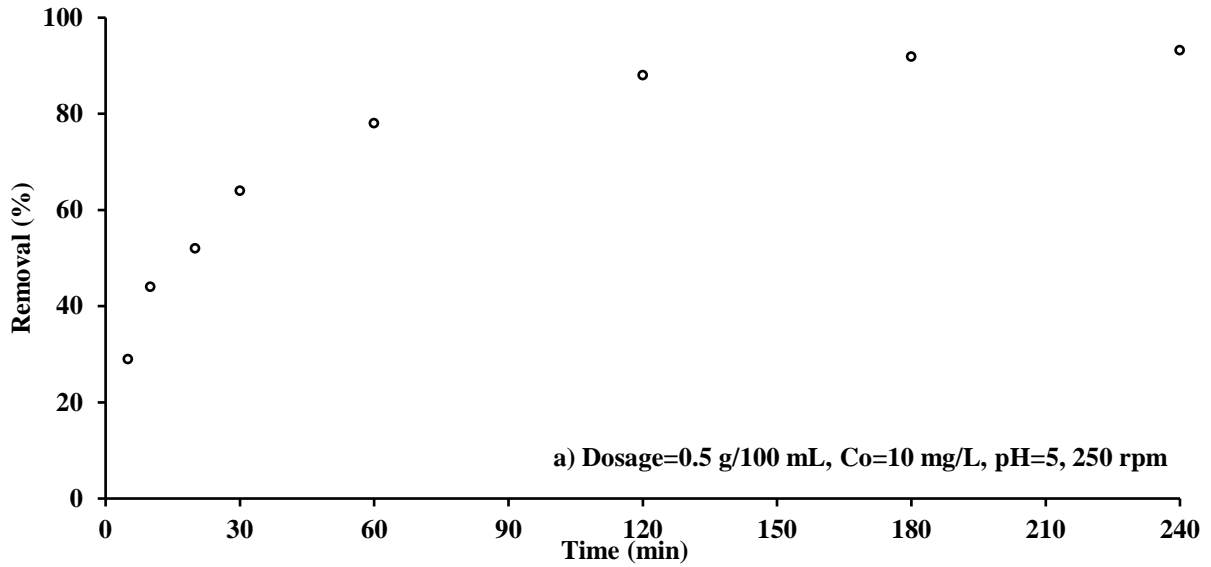


Figure 2. Effect of a) pH, b) Mg/Fe ratio, and c) dosage Mg/Fe-LDH on preparing sorbent for sorption of Pb ions



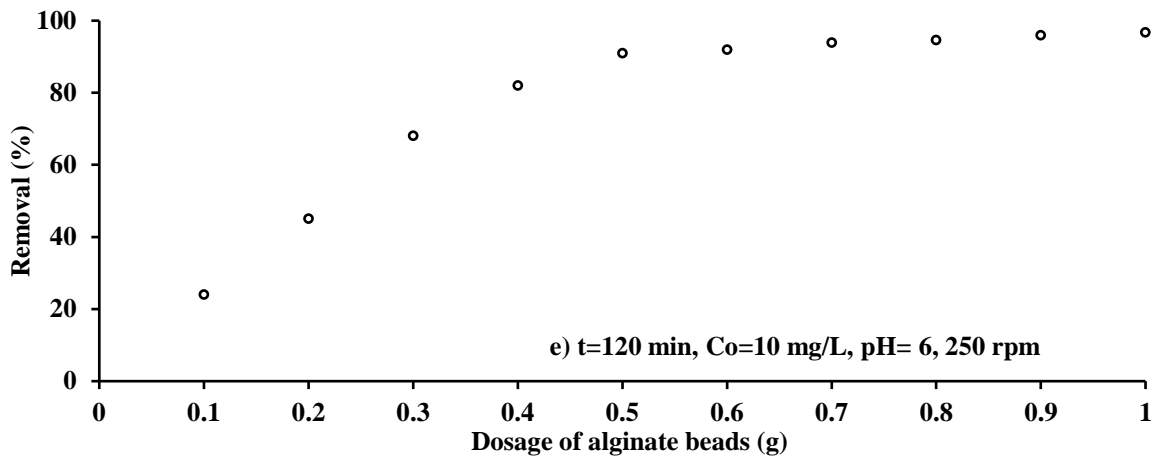


Figure 3. The impact of (a) contact time, (b) initial concentration, (c) agitation speed, (d) initial pH, and (e) alginate Mg/Fe-LDH-Na alginate beads dosage on removing Pb ions

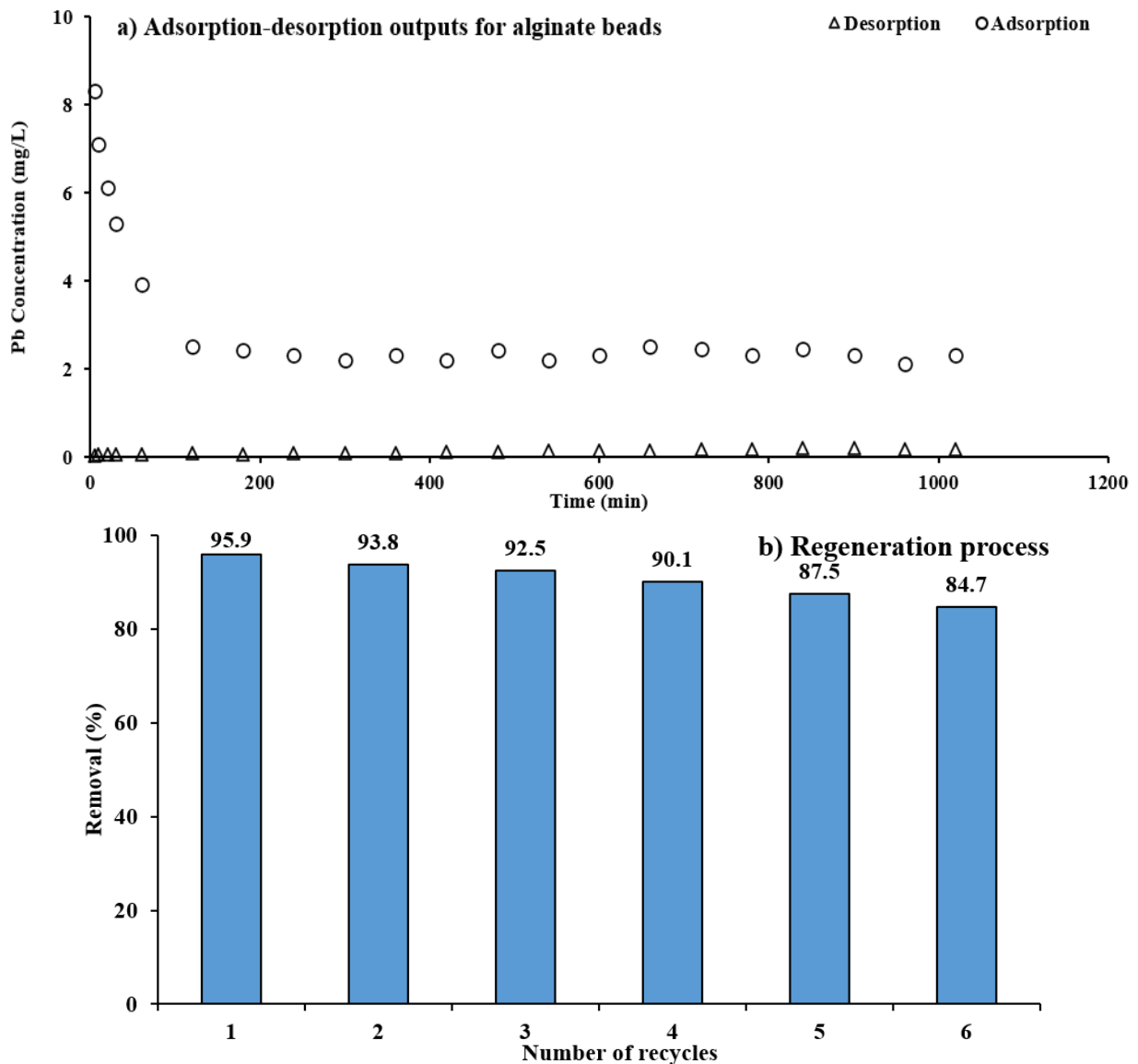


Figure 4. The outputs of (a) sorption-desorption outputs and (b) reusability of Mg/Fe-LDH beads for sorption of lead ions

The impact of adsorbent dosage on Pb ion adsorption was examined (0.1-1g) to determine the optimal dosage. According to Figure 3(e), the efficacy of Pb removal may rise with the bulk of the beads. This is evidenced by the increase in effective

regions with higher bead dosages [45, 46]. The sorption efficacy ranged from 24% to 96.7% due to changes in bead mass; 0.5 g seems to be the optimum dosage.

4.3 Leaching kinetics and reusability

To evaluate the prepared beads' potential and effectiveness, it is essential to investigate desorption properties. One gram of alginate beads was employed in 50 mL of water containing 10 mg/L of lead ions. The sorption results at pH 6, agitation 250 rpm over a contact time of 1020 minutes are plotted in Figure 4(a). Tests of desorption have been conducted by applying deionized water as the washing agent. The results, also shown in the same figure, indicate that Pb concentrations in the washing solution remained below 0.17 mg/L throughout the 1020-minute duration. These findings confirm the effectiveness of the prepared sorbent in capturing lead ions over an extended period, allowing for the exhausted Mg/Fe-LDH-Na alginate beads to be safely disposed of in sanitary landfills.

The feasibility of recycling the exhausted sorbent was investigated, and cycles of sorption and desorption must be conducted. The regeneration process involves using HCl (0.5 M) to desorb metal ions from adsorbent. Figure 4(b) illustrates the percentages of Pb removed in relation to the number of recycling cycles, demonstrating the effectiveness of the alginate beads in regeneration. Considering reusability is crucial, as it can significantly reduce operating costs and enhance the economic viability of the process for practical applications. The same conditions of batch adsorption experiments have maintained across five sequential cycles. As shown in Figure 4(b), the amount of lead removed in the first cycle was 95.9%. By the end of the six cycles, the capacity of the regenerated beads dropped to approximately 84.7%. This data indicates a decline in removal efficiencies with a higher number of cycles.

4.4 Characterization analyses

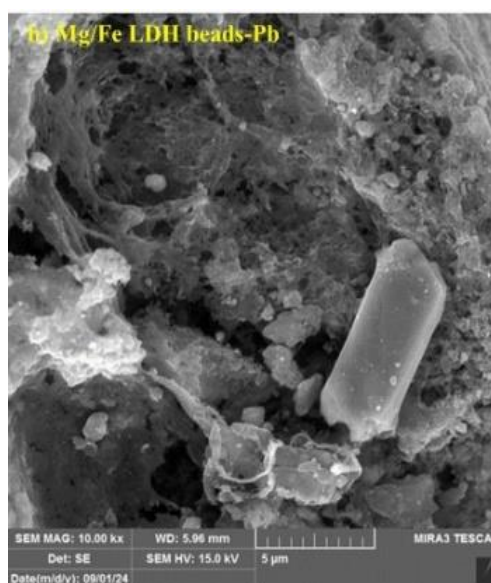
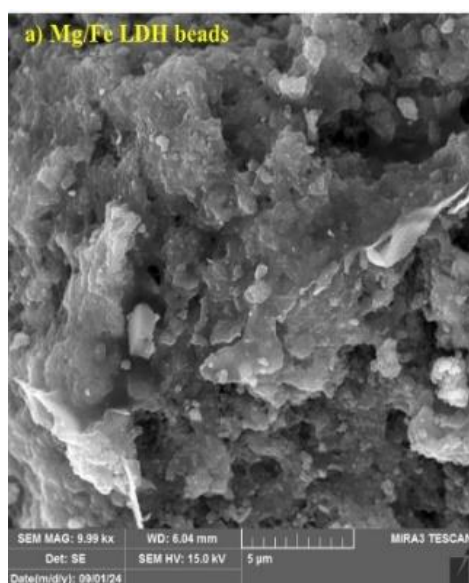
Fourier transform infrared (FT-IR) spectra of the sorbent, both before and after lead sorption, can be illustrated in Table 1 to identify the key functional groups responsible for metal ions sorption. The results indicate that amide and hydroxyl (-OH) groups undergo stretching vibrations, leading to the appearance of high-intensity absorption bands and complexation between Pb²⁺ ions and hydroxyl groups. The spectra reveal an absorption band in the frequency range of 3360-3456 cm⁻¹, attributed to the stretching modes of hydroxyl

groups and the stretching vibrations of hydrogen bonds. Additionally, a peak at 3360 cm⁻¹ corresponds to the stretching vibrations of -OH and C—H groups. Peaks observed at 1618 and 1423 cm⁻¹ are associated with O—H stretching vibrations and symmetric stretching vibrations of -COO, respectively. Weak bands at 1040 cm⁻¹ relate to the C-O stretching of COO⁻ and C-O-H groups, indicating coordination of Pb²⁺ ions with carboxylate groups, forming inner-sphere complexes [47, 48]. The absorption bands at 712 and 447 cm⁻¹ correspond to the stretching vibrations of Fe-O (from the ferrite skeleton) and Mg-O bonds, respectively. The slight shifts in Fe-O and Mg-O stretching vibrations imply possible ion exchange or surface complexation, where Pb²⁺ ions replace Fe or Mg in the LDH structure or bind to oxygen atoms [49].

Table 1. Functional groups and vibration types for sorption of Pb ions onto adsorbent

Band (cm ⁻¹)		Functional Group	Vibration Type	Intensity
Before Sorption	After Sorption			
3360	3456	-OH	Stretching, H-bonded	Strong, broad
1618	1607	O-H	Stretching	Strong
1423	1408	COO ⁻	Symmetric stretching	Strong
1040	1034	C-O	Stretching	Moderate
712	700	Fe-O	Stretching	Weak
447	430	Mg-O	Stretching	Strong

SEM-EDS analysis was used to characterize the surface properties of the prepared beads before and after contact with lead ions. Figure 5(a, b) shows the particle size, revealing that the adsorbent surfaces of the prepared beads exhibit a non-homogeneous morphology. At a 5 μm magnification scale, the surface appears highly compact and disordered. The Mg/Fe-LDH beads exhibit a micro-porous surface structure, which facilitates the adsorption of oxyanions. When comparing the Mg/Fe-LDH beads before and after the sorption process, significant changes in the bead morphology are observed following the removal of lead ions. EDS spectra provide insight into the changes in the elemental composition of the alginate beads, as shown in Figure 5(c, d). This figure explains the appearance of lead in the composition of beads at the end of the sorption process.



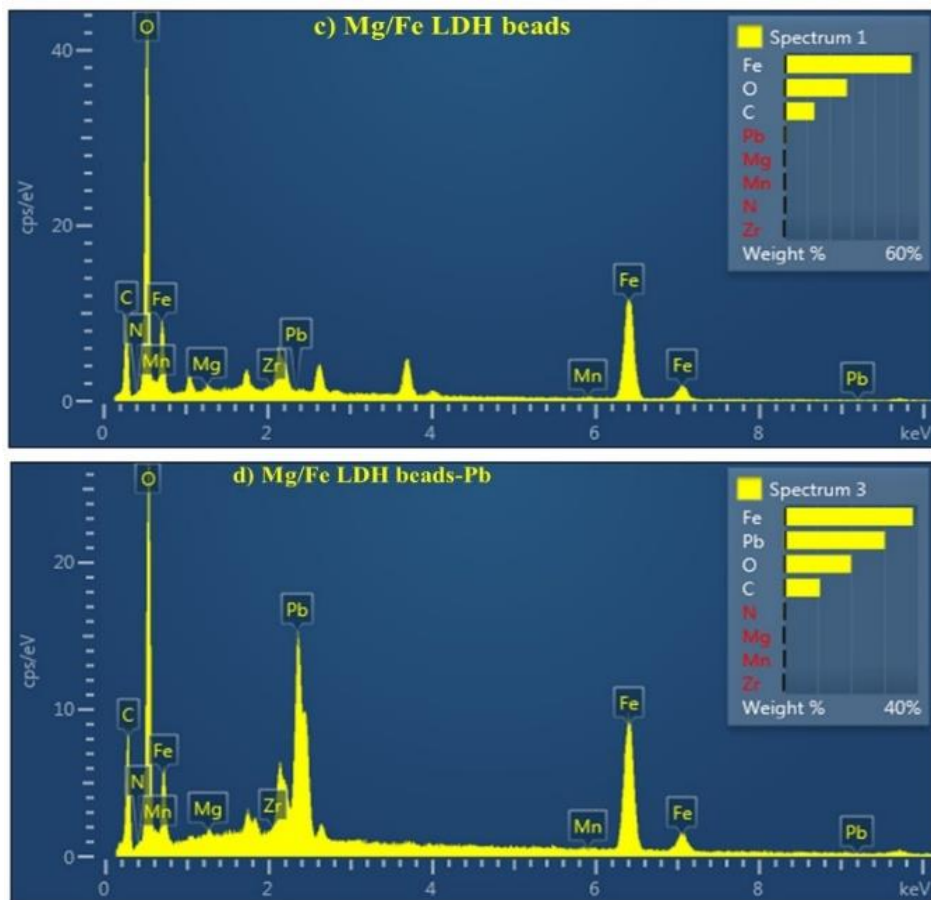


Figure 5. Characterization of the adsorbent using (a, b) SEM and (c, d) EDS analysis, before and after adsorption Pb ions

4.5 Isotherm and kinetics of sorption measurements

The adsorption equilibrium results from Pb adsorption onto the adsorbent have been analyzed using the sorption isotherm models previously discussed. The parameters for the Freundlich and Langmuir models are shown in Table 2, following the fitting of these models to the equilibrium sorption data shown in Figure 6(a) using Excel's nonlinear regression tool. The models' performance in comparison to the experimental data is shown in this graph. It is clear from Table 2 and Figure 6(a) that the "Langmuir model" fits and represents the adsorption mechanism more accurately than the "Freundlich model" since it has a greater "determination coefficient, R^2 ". This implies that the Pb ions are mostly sorbed as a monolayer on the surface of the beads. This implies uniform active sites across the adsorbent surface, each with equal affinity for lead ions. The Langmuir model indicates that the highest sorption capacity is 2.312 mg/g. This value is higher than those reported for other adsorbents, such as banana peels (2.2 mg/g), brown seaweed (1.4 mg/g), and fly ash bagasse (2.5 mg/g) [50, 51].

As shown in Figure 6(b), "pseudo-first-order and pseudo-second-order models" were used to formulate the sorption kinetics. Analysis of non-linear regression was conducted using Microsoft Excel 2016 to fit kinetic models with the experimental data. Table 2 includes the parameters of kinetic models as well as R^2 with "sum of square errors, SSE". The greater R^2 and lower SSE in this table show that the Pb adsorption kinetics is fitted with the pseudo-second-order models. This implies that the metal ions and alginate beads can be bonded by chemical forces.

Table 2. Parameters of isotherm and kinetic models for the sorption of Pb ions onto the adsorbent

Model	Parameter	Value
Freundlich	K_f (mg/g) (L/mg) ^{1/n}	1.433
	n	4.345
	R^2 , SSE	0.905, 0.166
Langmuir	q_{max} (mg/g)	2.312
	b (L/mg)	1.928
	R^2 , SSE	0.982, 0.029
Pseudo-first order	q_e (mg/g)	1.804
	k_1 (1/min)	0.051
Pseudo-second order	R^2 , SSE	0.977, 0.093
	q_e (mg/g)	1.988
	k_2 (g/mg min)	0.035
Intra-particle diffusion	Portion 1	
	k_{int} (mg/g min ^{0.5})	0.2407
	R^2	0.978
	Portion 2	
	k_{int} (mg/g min ^{0.5})	0.106
	R^2	0.933
Portion 3		
k_{int} (mg/g min ^{0.5})	0.0232	
R^2	0.947	

The intra-particle diffusion model (Figure 6(c) and Table 2) has further examined the kinetic observations and found a linear relation between q_t and $t^{0.5}$ with reasonable R^2 values. Three linear portions are represented by the plotted lines, indicating that two or more processes are involved in the sorption process. According to Table 2, the slopes of these lines represent the rate constants (k), with greater values for "portion 1" than for "portions 2 and 3". This suggests that

"instantaneous" or "external surface" sorption mechanisms control "portion 1". There are multiple separate portions (processes) in the Pb ions sorption can be recognized as follows:

- Portion 1: This initial phase is characterized by external mass transfer, where pb ions move from the pb solution to the adsorbent.
- Portion 2: This phase includes the diffusion of Pb ions into

the pores of the adsorbent.

- Portion 3: Equilibrium is reached between pb ions concentration in the water and on the adsorbent.

Based on the slopes of straight lines, the values of k_1 , k_2 , and k_3 , which stand for the rate constants for each phase, were calculated and listed in Table 2. The deviation from the origin indicates that diffusion limitations restrict the sorption rate [52].

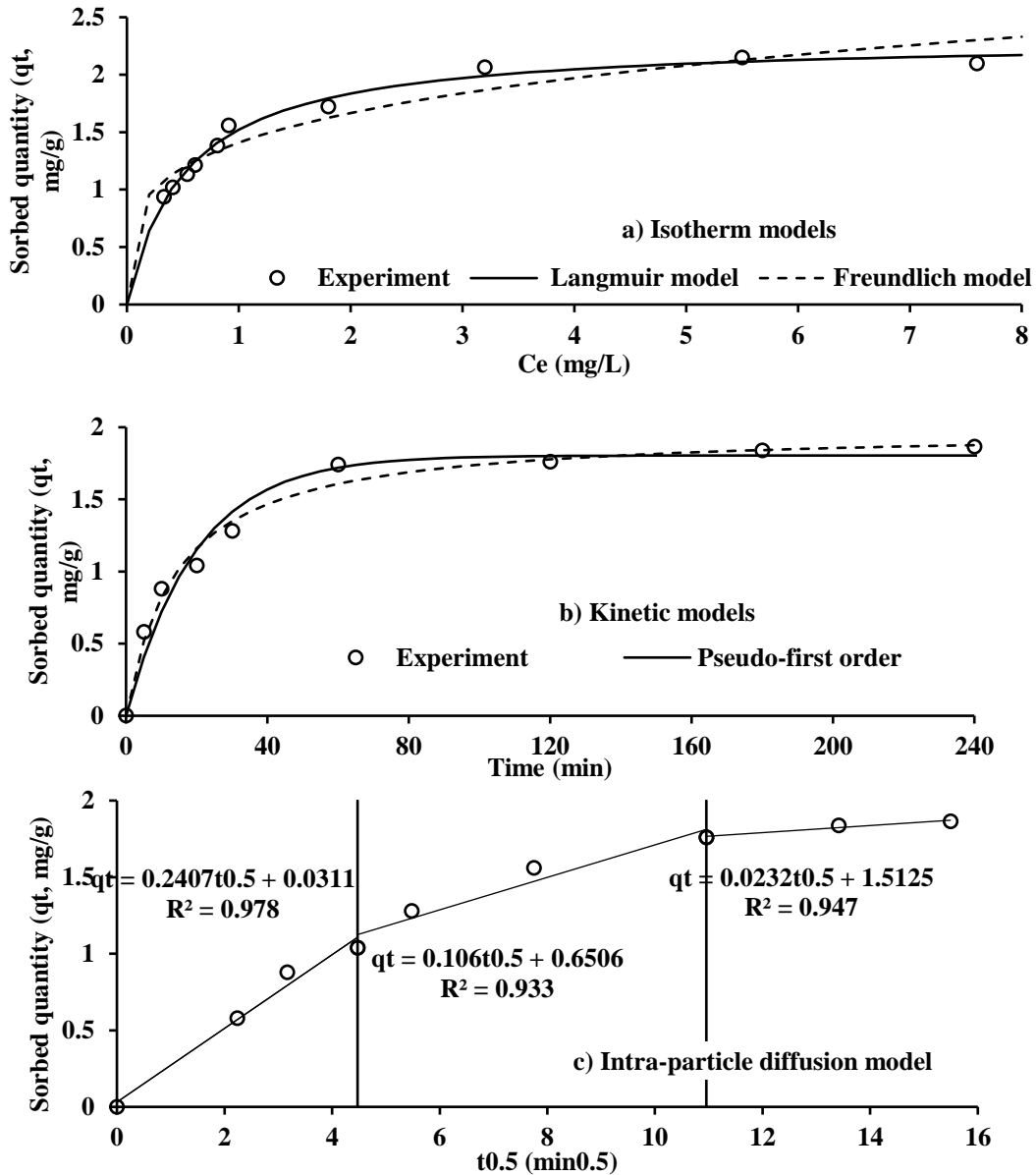


Figure 6. Concurrence between a) isotherms, b) kinetic, and c) intra-particle diffusion modes and sorption measurements for the interaction of Pb ions and prepared beads

5. CONCLUSIONS

Schanginia aegyptica and scrap iron (as solid waste) were successfully used as sources of Mg and Fe ions. The ions must be combined to produce Mg/Fe-LDH nanoparticles via the precipitation process. Utilizing such wastes can represent the real step in the application of sustainable ideas. Sodium alginate must be used to immobilize the generated nanoparticles to create spherical beads. The capacity of the spherical beads to remove Pb ions from aqueous solution was evaluated by batch studies. The optimal parameters for bead

synthesis are a mass of 5 grams of nanoparticles per 100 milliliters, a pH =10, and a (Mg/Fe) molar ratio = 3. The results showed that for C_0 10 mg/L at 250 rpm, the proper conditions needed to ensure the Pb ions elimination > 90% are time 120 min, pH 6, and dose 0.5 gram per 100 mL. The sorption interaction can be represented by the Langmuir model with a high capacity = 2.312 mg/g. The application of the "pseudo-second-order model" produced results that demonstrated the presence of chemical forces between Pb ions and beads. Characterization studies confirm the synthesis of magnesium/iron-LDH nanoparticles within the beads. EDS

analysis further revealed the incorporation of Pb ions into the bead composition following the sorption process.

REFERENCES

- [1] Aziz, K.H.H., Mustafa, F.S., Omer, K.M., Hama, S., Hamarawf, R.F., Rahman, K.O. (2023). Heavy metal pollution in the aquatic environment: Efficient and low-cost removal approaches to eliminate their toxicity: A review. *RSC Advances*, 13(26): 17595-17610. <https://doi.org/10.1039/D3RA00723E>
- [2] Ahmed, J.Y., Alrubaye, R.T.A. (2022). Gas adsorption and storage at metal-organic frameworks. *Journal of Engineering*, 28(1): 65-75. <https://doi.org/10.31026/j.eng.2022.01.05>
- [3] Ebrahim, S.E., Alhares, H.S. (2015). Competitive Removal of Cu^{2+} , Cd^{2+} and Ni^{2+} by Iron Oxide Nanoparticle (Fe_3O_4). *Journal of Engineering*, 21(4): 98-122. <https://doi.org/10.31026/j.eng.2015.04.06>
- [4] Hummadi, K. K. (2021). Optimal operating conditions for adsorption of heavy metals from an aqueous solution by an agriculture waste. *Iraqi Journal of Chemical and Petroleum Engineering*, 22(2): 27-35. <https://doi.org/10.31699/IJCPE.2021.2.4>
- [5] Flora, G., Gupta, D., Tiwari, A. (2012). Toxicity of lead: A review with recent updates. *Interdisciplinary Toxicology*, 5(2): 47-58. <https://doi.org/10.2478/v10102-012-0009-2>
- [6] Abdel Majeed, B.A., Muhseen, R.J., Jassim, N.J. (2017). Adsorption of mefenamic acid from water by bentonite poly urea formaldehyde composite adsorbent. *Journal of Engineering*, 23(7): 50-73. <https://doi.org/10.31026/j.eng.2017.07.04>
- [7] Hadi, H.S., Abd Ali, Z.T. (2024). Green approach for the synthesis of nanocomposite used as reactive material to containment amoxicillin and lead in groundwater. *Case Studies in Chemical and Environmental Engineering*, 9: 100707. <https://doi.org/10.1016/j.csee.2024.100707>
- [8] Ali, Q.A., Ali, M.F., Mohammed, S.J., M-Ridha, M.J. (2025). Utilising date palm fibres as a permeable reactive barrier to remove methylene blue dye from groundwater: A batch and continuous adsorption study. *Environmental Monitoring and Assessment*, 197: 166. <https://doi.org/10.1007/s10661-024-13603-0>
- [9] Li, B., Deng, Z., Lin, X., Chen, W., Li, P., Wu, J. (2024). Improved Pb(II) removal by D001 resin with a facile nanoscale α -FeOOH modification. *Journal of Environmental Chemical Engineering*, 12(2): 112468. <https://doi.org/10.1016/j.jece.2024.112468>
- [10] Ali, Z.T.A., Abdulhusain, N.A. (2023). Containment of ciprofloxacin and copper in groundwater using nanocomposite prepared by the use of pomegranate peel extract: Characterization, kinetic, and modeling study. *Desalination and Water Treatment*, 315: 327-341. <https://doi.org/10.5004/dwt.2023.30139>
- [11] Ammar, S.H., Khadim, H.J., Mohamed, A.I. (2018). Cultivation of *nannochloropsis oculata* and *isochrysis galbana* microalgae in produced water for bioremediation and biomass production. *Environmental Technology & Innovation*, 10: 132-142. <https://doi.org/10.1016/j.eti.2018.02.002>
- [12] Elmoubarki, R., Mahjoubi, F.Z., Tounsadi, H., Moustadraf, J., Abdennouri, M., Zouhri, A., Albani, A., El, Barka, N. (2015). Adsorption of textile dyes on raw and decanted Moroccan clays: Kinetics, equilibrium and thermodynamics, *Water Resources and Industry*, 9: 16-29. <https://doi.org/10.1016/j.wri.2014.11.001>
- [13] Alijamal, M., Ali, A.O. (2020). Lead reactions in some calcareous soils of northern Iraq. *Mesopotamia Journal of Agriculture*, 47(4): 8-26. <https://doi.org/10.33899/magrj.2020.126310.1015>
- [14] Rivera-Utrilla, J., Bautista-Toledo, I., Ferro-García, M.A., Moreno-Castilla, C. (2001). Activated carbon surface modifications by adsorption of bacteria and their effect on aqueous lead adsorption. *Journal of Chemical Technology & Biotechnology*, 76(12): 1209-1215. <https://doi.org/10.1002/jctb.506>
- [15] Adebowale, K.O., Unuabonah, I.E., Olu-Owolabi, B.I. (2006). The effect of some operating variables on the adsorption of lead and cadmium ions on kaolinite clay. *Journal of Hazardous Materials*, 134(1-3): 130-139. <https://doi.org/10.1016/j.jhazmat.2005.10.056>
- [16] Al, J.A.J.M.Z., Merkel, H.B.J., Awadh, S.M., Ibrahiem, O.S. (2016). Natural attenuation modelling of heavy-metal in groundwater of Kirkuk City, Iraq. *Iraqi Journal of Science*, 57(3B): 2043-2061.
- [17] Oubagaranadin, J.U.K., Murthy, Z.V.P. (2009). Adsorption of divalent lead on a montmorillonite-illite type of clay. *Industrial & Engineering Chemistry Research*, 48(23): 10627-10636. <https://doi.org/10.1021/ie9005047>
- [18] Liu, W.X., Song, S., Ye, M.L., Zhu, Y., Zhao, Y.G., Lu, Y. (2022). Nanomaterials with excellent adsorption characteristics for sample pretreatment: A review. *Nanomaterials*, 12(11): 1845. <https://doi.org/10.3390/nano12111845>
- [19] Ghosh, N., Das, S., Biswas, G., Haldar, P.K. (2022). Review on some metal oxide nanoparticles as effective adsorbent in wastewater treatment. *Water Science and Technology*, 85(12): 3370-3395. <https://doi.org/10.2166/wst.2022.153>
- [20] Sadegh, H., Ali, G.A.M., Gupta, V.K., Makhlof, A.S.H., Shahryari-ghoshekandi, R., Nadagouda, M.N., Sillanpää, M., Megiel, E. (2017). The role of nanomaterials as effective adsorbents and their applications in wastewater treatment. *Journal of Nanostructure in Chemistry*, 7: 1-14. <https://doi.org/10.1007/s40097-017-0219-4>
- [21] Alanazi, A.G., Habila, M.A., AlOthman, Z.A., Badjah-Hadj-Ahmed, A.Y. (2024). Synthesis and characterization of zinc oxide nanoparticle anchored carbon as hybrid adsorbent materials for effective heavy metals uptake from wastewater. *Crystals*, 14(5): 447. <https://doi.org/10.3390/cryst14050447>
- [22] Fan, L., Luo, C., Sun, M., Li, X., Qiu, H. (2013). Highly selective adsorption of lead ions by water-dispersible magnetic chitosan/graphene oxide composites. *Colloids and Surfaces B: Biointerfaces*, 103: 523-529. <https://doi.org/10.1016/j.colsurfb.2012.11.006>
- [23] Zhao, X., Jia, Q., Song, N., Zhou, W., Li, Y. (2010). Adsorption of Pb(II) from an aqueous solution by titanium dioxide/carbon nanotube nanocomposites: kinetics, thermodynamics, and isotherms. *Journal of Chemical & Engineering Data*, 55(10): 4428-4433. <https://doi.org/10.1021/je100586r>
- [24] Liang, X., Hou, W., Xu, Y., Sun, G., Wang, L., Sun, Y., Qin, X. (2010). Sorption of lead ion by layered double hydroxide intercalated with

- diethylenetriaminepentaacetic acid. *Colloids and Surfaces A: Physicochemical and Engineering Aspects*, 366(1-3): 50-57. <https://doi.org/10.1016/j.colsurfa.2010.05.012>
- [25] Abdel Moaty, S.A., Mahmoud, R.K., Mohamed, N.A., Gaber, Y., Farghali, A.A., Abdel Wahed, M.S.M., Younes, H.A. (2019). Synthesis and characterisation of LDH-type anionic nanomaterials for the effective removal of doxycycline from aqueous media. *Water and Environment Journal*, 34(S1): 290-308. <https://doi.org/10.1111/wej.12526>
- [26] Yang, Z., Yan, H., Yang, H., Li, H., Li, A., Cheng, R. (2013). Flocculation performance and mechanism of graphene oxide for removal of various contaminants from water. *Water Research*, 47(9): 3037-3046. <https://doi.org/10.1016/j.watres.2013.03.027>
- [27] Li, S.S., Jiang, M., Jiang, T.J., Liu, J.H., Guo, Z., Huang, X.J. (2017). Competitive adsorption behavior toward metal ions on nano-Fe/Mg/Ni ternary layered double hydroxide proved by XPS: Evidence of selective and sensitive detection of Pb(II). *Journal of Hazardous Materials*, 338: 1-10. <https://doi.org/10.1016/j.jhazmat.2017.05.017>
- [28] Sun, J., Chen, Y., Yu, H., Yan, L., Du, B., Pei, Z. (2018). Removal of Cu²⁺, Cd²⁺ and Pb²⁺ from aqueous solutions by magnetic alginate microsphere based on Fe₃O₄/MgAl-layered double hydroxide. *Journal of Colloid and Interface Science*, 532: 474-484. <https://doi.org/10.1016/j.jcis.2018.07.132>
- [29] Mahmoudi, S., Chemat-Djenni, Z., Bouguettoucha, A., Guediri, A., Chebli, D., Gil, A. (2022). Removal of Pb (II) from aqueous solutions by new layered double hydroxides adsorbent MgCuCaAl-LDH: Free gibbs energy, entropy and internal energy studies. *Inorganic Chemistry Communications*, 144: 109910. <https://doi.org/10.1016/j.inoche.2022.109910>
- [30] Wang, H., Lin, T., He, T., An, S., Chen, W., Song, Y.F. (2025). Simultaneous super-stable mineralization of Pb²⁺, Cd²⁺ and Cu²⁺ using MIL-101(Fe)@MgFe-LDH. *Separation and Purification Technology*, 353: 128263. <https://doi.org/10.1016/j.seppur.2024.128263>
- [31] Kiani, M., Bagherzadeh, M., Ghadiri, A.M., Makvandi, P., Rabiee, N. (2022). Multifunctional green synthesized Cu–Al layered double hydroxide (LDH) nanoparticles: Anti-cancer and antibacterial activities. *Scientific Reports*, 12: 9461. <https://doi.org/10.1038/s41598-022-13431-7>
- [32] Soltani, R., Pelalak, R., Pishnamazi, M., Marjani, A., Albadarin, A.B., Sarkar, S.M., Shirazian, S. (2021). A novel and facile green synthesis method to prepare LDH/MOF nanocomposite for removal of Cd(II) and Pb(II). *Scientific Reports*, 11: 1609. <https://doi.org/10.1038/s41598-021-81095-w>
- [33] Osman, A.I., Zhang, Y., Farghali, M., Rashwan, A.K., Eltaweil, A.S., Abd El-Monaem, E.M., Mohamed, I.M.A., Badr, M.M., Ihara, I., Rooney, D.W., Yap, P.S. (2024). Synthesis of green nanoparticles for energy, biomedical, environmental, agricultural, and food applications: A review. *Environmental Chemistry Letters*, 22: 841-887. <https://doi.org/10.1007/s10311-023-01682-3>
- [34] Yaseen, R.A.A., Ibrahim, M.A., Ahmed, M. (2022). The effect of Schanginia aegyptica and Urtica dioica powder on the growth of Trigonella foenum seedlings in laboratory sterilized soil. *HIV Nursing*, 22: 243-247.
- [35] Rashid, H.M., Faisal, A.A.H. (2018). Removal of dissolved cadmium ions from contaminated wastewater using raw scrap zero-valent iron and zero valent aluminum as locally available and inexpensive sorbent wastes. *Iraqi Journal of Chemical and Petroleum Engineering*, 19(4): 39-45. <https://doi.org/10.31699/IJCPE.2018.4.5>
- [36] Weber, W.J., Morris, J.C. (1962). Advances in water pollution research: Removal of biologically resistant pollutant from waste water by adsorption. In *Proceedings of the International Conference on Water Pollution Symposium*, 2: 231-266.
- [37] Lucas, S., Cocero, M.J., Zetzi, C., Brunner, G. (2004). Adsorption isotherms for ethylacetate and furfural on activated carbon from supercritical carbon dioxide. *Fluid Phase Equilibria*, 219(2): 171-179. <https://doi.org/10.1016/j.fluid.2004.01.034>
- [38] Qiu, H., Lv, L., Pan, B., Zhang, Q., Zhang, W., Zhang, Q. (2009). Critical review in adsorption kinetic models. *Journal of Zhejiang University-SCIENCE A*, 10: 716-724. <https://doi.org/10.1631/jzus.A0820524>
- [39] McKay, G., Porter, J.F., Prasad, G.R. (1999). The removal of dye colours from aqueous solutions by adsorption on low-cost materials. *Water, Air, and Soil Pollution*, 114: 423-438. <https://doi.org/10.1023/A:1005197308228>
- [40] Wang, S., Wang, H. (2015). Adsorption behavior of antibiotic in soil environment: A critical review. *Frontiers of Environmental Science & Engineering*, 9: 565-574. <https://doi.org/10.1007/s11783-015-0801-2>
- [41] Park, J.B., Lee, S.H., Lee, J.W., Lee, C.Y. (2002). Lab scale experiments for permeable reactive barriers against contaminated groundwater with ammonium and heavy metals using clinoptilolite (01-29B). *Journal of Hazardous Materials*, 95(1-2): 65-79. [https://doi.org/10.1016/S0304-3894\(02\)00007-9](https://doi.org/10.1016/S0304-3894(02)00007-9)
- [42] Elkady, M.F., Mahmoud, M.M., Abd-El-Rahman, H.M. (2011). Kinetic approach for cadmium sorption using microwave synthesized nano-hydroxyapatite. *Journal of Non-Crystalline Solids*, 357(3): 1118-1129. <https://doi.org/10.1016/j.jnoncrysol.2010.10.021>
- [43] Asaoka, S., Kawakami, K., Saito, H., Ichinari, T., Nohara, H., Oikawa, T. (2021). Adsorption of phosphate onto lanthanum-doped coal fly ash—Blast furnace cement composite. *Journal of Hazardous Materials*, 406: 124780. <https://doi.org/10.1016/j.jhazmat.2020.124780>
- [44] Hawal, L., Al-Sulttani, A., Kariem, N. (2021). Adsorption of lead ions from aqueous solutions onto rice husks, continuous system. *Journal of Ecological Engineering*, 22(10): 269-274. <https://doi.org/10.12911/22998993/141936>
- [45] Ge, M., Du, M., Zheng, L., Wang, B., Zhou, X., Jia, Z., Hu, G., Jahangir Alam, S.M. (2017). A maleic anhydride grafted sugarcane bagasse adsorbent and its performance on the removal of methylene blue from related wastewater. *Materials Chemistry and Physics*, 192: 147-155. <https://doi.org/10.1016/j.matchemphys.2017.01.063>
- [46] Hussain, A., I Al-Jeboori, M., Munan Yaseen, H. (2007). Adsorption of Cobalt (II) ion from Aqueous Solution on Selected Iraqi clay surfaces. *Journal of Kerbala University*, 3(2): 20-38.
- [47] Islam, M., Ahmed, N., Hossain, M., Rahman, A., Sultana,

- A. (2016). Effect of pH on the adsorption kinetics of Cr(VI) on sodium chlorite treated coconut coir. *Bangladesh Journal of Scientific and Industrial Research*, 51(2): 95-100. <https://doi.org/10.3329/bjsir.v51i2.28090>
- [48] Faisal, A.A.H., Al-Ridah, Z.A., Naji, L.A., Naushad, M., El-Serehy, H.A. (2020). Waste foundry sand as permeable and low permeable barrier for restriction of the propagation of lead and nickel ions in groundwater. *Journal of Chemistry*, 2020(1): 1-13. <https://doi.org/10.1155/2020/4569176>
- [49] Ahmed, D.N., Naji, L.A., Faisal, A.A.H., Al-Ansari, N., Naushad, M. (2020). Waste foundry sand/MgFe-layered double hydroxides composite material for efficient removal of Congo red dye from aqueous solution. *Scientific Reports*, 10: 2042. <https://doi.org/10.1038/s41598-020-58866-y>
- [50] Chowdhury, I.R., Chowdhury, S., Mazumder, M.A.J., Al-Ahmed, A. (2022). Removal of lead ions (Pb²⁺) from water and wastewater: A review on the low-cost adsorbents. *Applied Water Science*, 12: 185. <https://doi.org/10.1007/s13201-022-01703-6>
- [51] Vieira, D.M., da Costa, A.C.A., Henriques, C.A., Cardoso, V.L., Pessoa de Franca, F. (2007). Biosorption of lead by the brown seaweed *Sargassum filipendula* - batch and continuous pilot studies. *Electronic Journal of Biotechnology*, 10(3). <https://doi.org/10.2225/vol10-issue3-fulltext-3>
- [52] Cheung, W.H., Szeto, Y.S., McKay, G. (2007). Intraparticle diffusion processes during acid dye adsorption onto chitosan. *Bioresource Technology*, 98(15): 2897-2904. <https://doi.org/10.1016/j.biortech.2006.09.045>